

Experimental and Theoretical Study of Coating Spalling under High-Cycle Frictional Loading

E. V. Torskaya^{1*}, A. M. Mezrin¹, I. V. Mosyagina², and Yu. V. Kornev³

¹ *Institute for Problems in Mechanics, Russian Academy of Sciences, Moscow, 119526 Russia*

² *All-Russian Research Institute of Chemical Technology, Moscow, 115409 Russia*

³ *Institute of Applied Mechanics, Russian Academy of Sciences, Moscow, 125040 Russia*

* e-mail: torskaya@mail.ru

Received July 13, 2016, revised July 13, 2016, accepted August 22, 2016

Abstract—An experimental and theoretical study of contact fatigue damage accumulation at the coating–substrate interface has been carried out for the case of frictional contact between a smooth coating and a rough counterbody. Coatings were synthesized via low-temperature thermal decomposition of metal (Al, Zr) carboxylate solutions, which resulted in the formation of nanoscale amorphous nanocrystalline oxide layers 20–400 nm thick (depending on the concentration of the film-forming solution and the number of loading cycles) on the substrate surface (quartz glass). The investigation included coating deposition, determination of coating mechanical properties by indentation, development of the friction test procedure, stress calculation at the coating–substrate interface by modeling high-cyclic frictional loading, and the choice of a damage accumulation model for the coating–substrate interface that relates the stress state to the number of cycles to coating spalling. Preliminary tests revealed the coating compositions and coating deposition techniques that provide the highest spalling resistance under cyclic contact loading. Parameters in the relation for contact fatigue damage accumulation were determined and the model was verified by analyzing the experimental load dependence of the number of cycles to coating spalling on the microscale. It has been shown that the linear damage summation model conventionally used for describing failure due to fatigue damage accumulation in some materials can be applied to investigate the coating–substrate interface whose properties depend not only on the properties of the interfacing materials but also on the coating deposition technique.

DOI: 10.1134/S1029959918060012

Keywords: coating, contact problem, indentation, roughness, friction, contact fatigue failure

1. INTRODUCTION

The spalling of coatings in friction is an important issue in the mechanics of frictional interaction, and in the development of materials and coating deposition techniques for friction joints. There are two causes of failure at the coating–substrate interface: an increase above the threshold stresses, and a cyclic variation of stress fields in frictional interaction that leads to failure by a fatigue mechanism. A standard method for estimating the coating adhesion to the substrate is a scratch test that reveals the threshold stress values, the surpassing of which causes contact failure. Unfortunately, there are no similar standard methods of durability estimation for coatings that peel off by the contact fatigue mechanism. Some authors studied experimentally the contact fatigue failure of thick coatings [1, 2], but without considering

spalling of these coatings. One of the main reasons for the absence of such studies is the time consuming experiments. On the other hand, thin coating deposition techniques are currently being developed in which the coating thickness is comparable to the size of the contact spots due to roughness. There is a high stress concentration near the actual contact spots, including at the interface, and the migration of the actual contact spots with the relative motion of the surfaces is accompanied by a cyclic change in the stress fields. The cyclic changes occur at the microlevel in this case and therefore the duration of the experiment can be significantly reduced.

The aim of this paper is to develop an experimental and theoretical method for studying contact fatigue failure (spalling) of thin (up to 0.5 μm) coatings in frictional contact with a specially prepared rough surface. The theoretical part is based on the previously developed [3–

5] methods for determining the stress state and the damage accumulation function in multiple frictional contacts.

2. MODELING OF CONTACT FATIGUE DAMAGE ACCUMULATION AT THE COATING–SUBSTRATE INTERFACE

The first stage of modeling included the stress state determination at the coating–substrate interface.

The rough surface was modeled by a periodic system of spherical indenters of radius R located in the sites of a hexagonal lattice with period l (Fig. 1). The system of indenters slides with a constant velocity along the boundary of a two-layered elastic half-space; the sliding direction coincides with the $0x$ axis direction. The system is loaded by the period-averaged pressure p_n and the tangential stresses τ_n , that balance the tangential stresses acting on the contact areas. These loading parameters are interrelated by the Coulomb–Amontons law, i.e., $\tau_n = \mu p_n$, where μ is the coefficient of sliding friction. When solving the contact problem, we assumed that the influence of the friction-induced surface tangential stresses on the normal stresses and displacements can be neglected.

The following conditions are fulfilled on the upper boundary of the coating ($z = H$):

$$w^{(1)}(x, y) + w^{(0)}(x, y) = f(x, y) - \delta, \quad (x, y) \in \omega_i,$$

$$\sigma_z^{(1)} = 0, \quad (x, y) \notin \omega_i, \quad i = 1, 2, \dots, \infty, \quad (1)$$

$$\tau_{xz}^{(1)} = 0, \quad \tau_{yz}^{(1)} = 0, \quad 0 \leq x < \infty, \quad 0 \leq y < \infty.$$

Here, $f(x, y)$ is the form of an arbitrary indenter, ω_i is the actual contact spot, and $w^{(1)}(x, y), w^{(0)}(x, y)$ are the

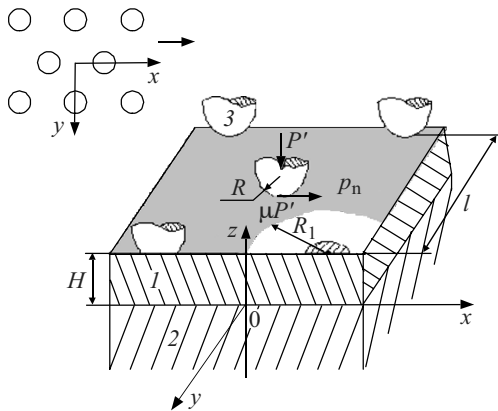


Fig. 1. Schematic of a frictional contact between a periodic system of indenters and a two-layer elastic half-space: 1—coating; 2—substrate; 3—indenter.

normal displacements of the coating surface and indenter surface, respectively.

The load P' applied to each indenter and the nominal pressure p_n are related by the ratio

$$P' = \pi R_1^2 p_n = \sqrt{3}/2 l^2 p_n. \quad (2)$$

The equilibrium equation is used in the form

$$P' = \iint_{\omega_i} p(x, y) ds, \quad (3)$$

where $p(x, y)$ is the contact pressure distribution.

The coating–substrate interface ($z = 0$) is assumed to be in the conditions of complete adhesion:

$$w^{(1)} = w^{(2)}, \quad v_x^{(1)} = v_x^{(2)}, \quad v_y^{(1)} = v_y^{(2)},$$

$$\sigma_z^{(1)} = \sigma_z^{(2)}, \quad \tau_{xz}^{(1)} = \tau_{xz}^{(2)}, \quad \tau_{yz}^{(1)} = \tau_{yz}^{(2)}. \quad (4)$$

The method of solving the contact problem with conditions (1)–(4) is described in Ref. [3]. It is based on the use of the localization method [6], the boundary element method, in which the influence coefficients are determined using the Hankel integral transforms [7], and an iterative procedure.

The obtained contact pressure distributions are then used to calculate the stresses arising in frictional contact. The following conditions are fulfilled at the upper boundary of the coating:

$$\sigma_z^{(1)}(x, y) = p(x, y), \quad \tau_{xz}^{(1)} = -\mu p(x, y), \quad (x, y) \in \omega_i,$$

$$\sigma_z^{(1)} = 0, \quad \tau_{xz}^{(1)} = 0, \quad (x, y) \notin \omega_i, \quad (5)$$

$$\tau_{yz}^{(1)} = 0, \quad 0 \leq x < \infty, \quad 0 \leq y < \infty.$$

The lower boundary of the layer is under boundary conditions (4).

The problem with boundary conditions (4), (5) is reduced to the determination of the internal stresses due to the constant distributed load and is solved by the method based on double integral Fourier transforms [7]. The contribution of the tangential forces acting on all contact spots to the layer stress state within one period was studied using an approach based on the principles of localization and superposition [3, 4]. By calculating the stress distribution at the interface between the elastic layer and the half-space, we determined the maximum stress amplitude values along the $0x$ axis that coincides with the sliding direction of the indenter system. It was assumed that the maximum amplitude values are in the plane passing through the geometric center of the contact area. As a result, the function $\Delta\tau_1$ is calculated for the layer–half-space interface, which determines the maximum amplitude values of the maximum tangential stresses and is independent of the coordinates.

The function $\Delta\tau_1$ is used as an input parameter for the modeling of contact fatigue failure at the coating–

substrate interface. The model employs a macroscopic approach [8, 9], i.e., a positive time nondecreasing function $Q(M, t)$ is defined which characterizes the material damage at an arbitrary point of the interface $M(x, y)$ and depends on the stress amplitude values at the given point. A linear damage summation model is used. Failure occurs in the time point t^* when the damage function reaches a specified threshold value. The rate of fatigue damage accumulation $\partial Q(x, y, t)/\partial t$ is related to the amplitude value $\Delta\tau_1$ of the maximum tangential stresses by the dependence [4, 6]:

$$q(x, y, t) = \frac{\partial Q(x, y, t)}{\partial t} = c(\Delta\tau_1(x, y, t))^m. \quad (6)$$

Here, c and m are the experimentally determined constants characterizing the strength properties of the interface.

Since the considered problem is periodic, the damage function does not depend on the x and y coordinates and is a function of only time t , which can be expressed in terms of the number of cycles N , i.e., $Q = Q(N)$:

$$Q(N) = \int_0^N q_n(n) dn + Q_0, \quad (7)$$

where Q_0 is the initial damage of the material, and $q_n(n)$ is the coordinate-independent damage accumulation rate.

Failure occurs when the critical damage value is reached. This condition can be written as follows:

$$Q(N^*) = 1, \quad (8)$$

where N^* is the number of cycles to failure.

With the assumption of linear damage summation at a zero initial damage value, Eq. (8) is written as

$$N^* c(\Delta\tau_1)^m = 1. \quad (9)$$

The values of N^* can be estimated experimentally, and the stress amplitude values can be determined from calculations for different load values. Therefore, we can find the values of the parameters c and m .

3. CONDITIONS FOR THE APPLICABILITY OF THE CONTACT FATIGUE DAMAGE ACCUMULATION MODEL FOR DESCRIBING AN EXPERIMENT ON COATING PEELING

The model proposed above can be applied to study experimentally and theoretically the strength properties of the coating–substrate interface, provided certain conditions are met.

A counterbody for friction tests must be rough, with single-level roughness of relatively periodic structure. In this case, the average values of the period and curvature

radius of the roughness can be used to construct a periodic model. Taking into account the relative sliding and a large number of cycles, this averaging is justified for use in a model that assumes a linear damage summation over each loading cycle.

The roughness of the coated substrate and the coating surface must be much smaller than the counterbody roughness. The coating thickness must be comparable with the size of the actual contact spots.

The value of the friction coefficient must be low to exclude the associated mechanisms of coating failure (microcutting, debris formation, temperature flashes causing structural changes, etc.).

Contact conditions at the macrolevel should be such that the nominal pressure can be calculated with regard to the compliance of the rough layer. The pin-on-disk contact is optimal because, as was shown in Ref. [6], the macroscopic pressure is well balanced due to the roughness, so that it can be considered constant with a small error.

The materials of the coating and the substrate should remain elastic in the considered stress ranges. The structure of the materials must be such that they can be considered homogeneous on the scale of the model.

4. METHOD OF OBTAINING THE COATING–SUBSTRATE COMPOSITION FOR EXPERIMENTAL RESEARCH

The investigated coatings were formed by low-temperature thermal decomposition of isomeric carboxylates of metals. The main stages of the process include the synthesis of film-forming solutions of individual metals (metal carboxylates), mixing of the metal carboxylates in the required proportion and their deposition on the substrate surface with the gravimetric control of the amount of film-forming solution, and thermolysis. Thermolysis can be carried out at different temperatures, which mainly determine the phase structure of the resulting coating. The thickness of a single oxide layer is 20–150 nm (depending on the solution concentration). For the synthesis of microsized coatings, the deposition–thermolysis procedures are repeated [10]. The substrate was made of quartz glass KUVI with small surface roughness. Our previous studies have shown [11, 12] that, unlike coatings on steel substrates, coatings on glass are free from defects and cracks induced by residual stresses.

The investigation was performed for an alumina and zirconia composition because the technology allows the synthesis of a ceramic two-component Al_2O_3 – ZrO_2 ma-

Table 1. Samples for preliminary tests

No.	1	2	3	4	5	6	7	8	9	10
Al:Zr	10:1	6:1	10:1	6:1	10:1	6:1	10:1	6:1	10:1	6:1
$T, ^\circ\text{C}$	600		700		700		800		800	
Thickness, nm	140		140		200		140		240	
Young's modulus, GPa	133	127	154	153	156	152	146	146	148	173
Number of cycles $\times 10^7$	1.2	1.2	0.4	0.5	0.8	0.8	0.5	0.6	0.6	1.2

terial known for its mechanical properties, such as strength, wear resistance, thermal and chemical stability [13]. The crystallite size in the synthesized coating is mainly determined by the temperature and time of heat treatment, which allows control over crystallite growth and thereby reduces the conditions for the formation of bulk structural defects [14]. Moreover, $\text{Al}_2\text{O}_3\text{-ZrO}_2$ coatings are eutectic. Their structural strength is provided inter alia by cracking inhibition at the interface of mutually inert phases, which ensures good adhesion between the substrate and the oxide layer.

Samples for preliminary studies differed in the proportion of oxides in their composition, and in the final finishing temperature and thickness (Table 1). Based on the preliminary tests, we chose the material for the main tests conducted on 18 identical samples.

5. METHOD FOR DETERMINATION OF ELASTIC PROPERTIES OF COATINGS BY INDENTATION RESULTS

Models for the calculation of the stress state and contact fatigue damage accumulation can be used if we know the elastic characteristics of the coating, substrate and counterbody materials. The Young's modulus of the

used quartz glass was calculated earlier and is equal to 110 GPa [11]. All samples for preliminary tests were examined by nanoindentation using a NanoTest 600 nano-indenter (MicroMaterials Ltd., UK).

It is assumed that when the Berkovich pyramid, which is currently the most common indenter head, is forced into the coating to a depth not exceeding 1/10 of the coating thickness, the influence of the substrate can be neglected and standard software designed for homogeneous bodies can be used. However, in the case of hard coatings, the indentation results must be interpreted taking into account the deformation of a softer substrate [15]. Earlier, we developed a method for calculating the elastic characteristics of thin hard coatings based on cone indentation with a known indenter tip radius [16]. In this study, the experiment was performed using a diamond cone indenter with a cone angle of 60° and a tip radius of $10\ \mu\text{m}$; the load resolution was $60\ \mu\text{N}$ and the penetration depth resolution was $0.04\ \text{nm}$. Indentation was carried out under controlled load, with a preload of $0.1\ \text{mN}$. The load-indentation depth curves were plotted during loading and unloading. The unloading rate was the same as the loading rate. A series of 10 experiments was conducted for different points on the surface. The maximum load was 5 and 10 mN.

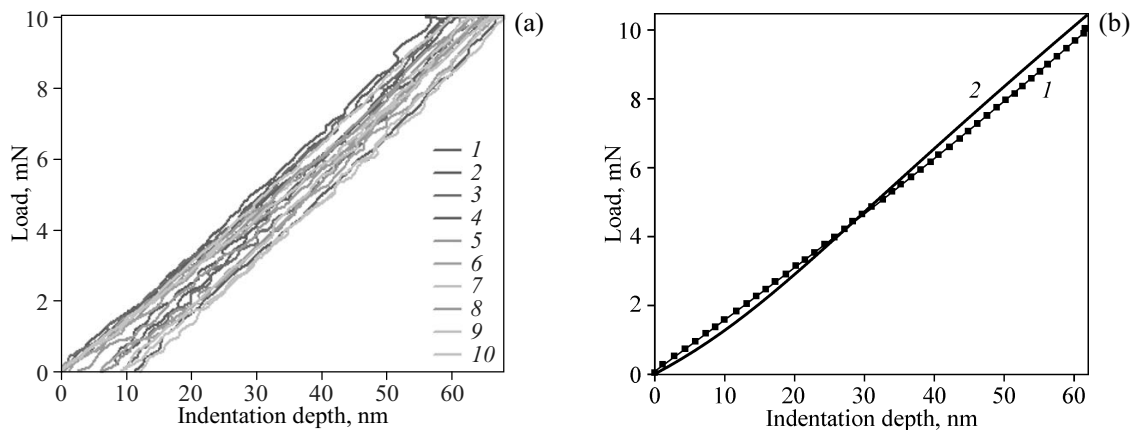


Fig. 2. Loading-unloading curves plotted in indentation of sample No. 9 (a); averaged experimental unloading curve (1) and calculated elastic indentation curve (2) with a coating elastic modulus of 148 GPa (b).

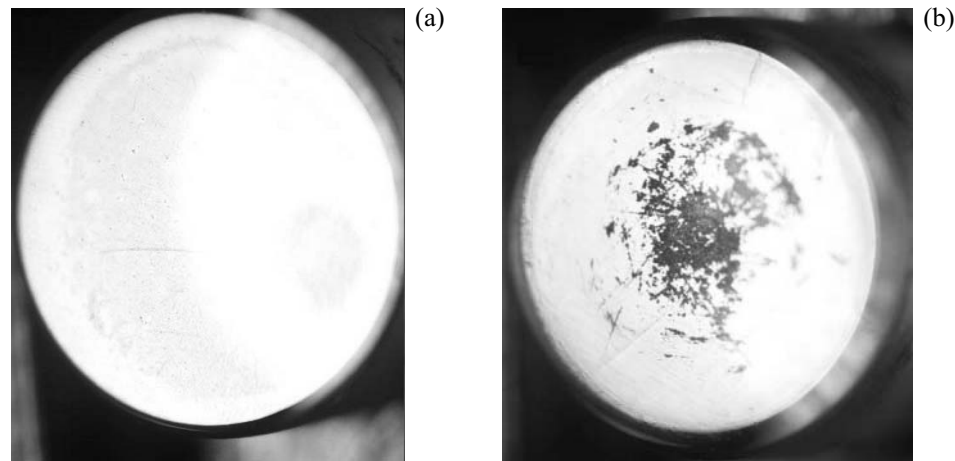


Fig. 3. Examined coatings before (a) and after testing (b).

The elastic modulus of the coating was calculated by solving a contact problem for a two-layer elastic half-space and a smooth indenter, which is a special case of the problem with boundary conditions (1)–(4). In this case, it is impossible to invert the problem in order to determine the unknown elastic modulus for known load and indentation depth values, because the form of the pressure distribution function is not known in advance. At the same time, it is possible to solve a series of contact problems with a varying elastic modulus, to plot the curve of indentation depth versus elastic modulus in the selected range and at a fixed load, and to choose the elastic modulus value that gives the experimental indentation depth value. With a large number of points on the unloading curve, we can obtain many elastic modulus values that are close within a small experiment and calculation error. The following algorithm was used: five out of ten unloading curves were selected to provide a minimum spread, and then the averaged experimental unloading curve was calculated to select ten points with different loads on it. The elastic modulus was calculated for these points and then the average value was determined.

As an example, Figure 2a illustrates the loading–unloading curves obtained for sample No. 9, and Figure 2b shows the averaged experimental unloading curves 1 and 2 obtained in modeling the elastic indentation of a cone indenter into the coating with regard to the deformation of the coating, substrate and indenter materials; the coating elastic modulus determined by the above described method was equal to 148 GPa.

The results of elastic modulus determination for all coating samples are given in Table 1.

6. CONTACT FATIGUE TESTING OF COATINGS

Reciprocating pin-on-disk tests were carried out on a UMT-3 tribometer (CETR) at a given speed. The principle of the tribometer operation is described in Ref. [17].

The pin was a cylinder of 6 mm in diameter made of quartz glass, coated with the studied coating on one of its ends (Fig. 3a). The counterbody was a steel bar measured $70 \times 20 \times 10 \text{ mm}^3$. Its wear face was ground on a rough stone and then polished. The polishing provided a relief on the counterbody whose surface profile (along the pin motion direction) is shown in Fig. 4. The average roughness density $m = 20 \text{ mm}^{-1}$.

The pin-on-disk test setup is shown in Fig. 5. The tests were carried out with the displacement amplitude $A = 7.5 \text{ mm}$ and the frequency $n = 10 \text{ Hz}$ with lubrication. The lubricant was added in the amount necessary to achieve a low friction coefficient and prevent microcutting, but to negate the effect of the roughness in the contact area. The lubricant material was synthetic diesel oil with a viscosity of 5W-40.

The coating spalling was examined visually every 5 min during the experiment after the friction process was stopped and the lubricant was wiped off from the



Fig. 4. Surface roughness profile of the counterbody.

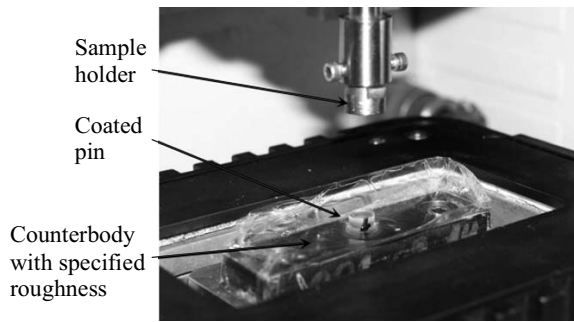


Fig. 5. Pin-on-disk test setup.

sample. If the coating remained intact, the sample was returned to the holder to continue the test. Otherwise, the experiment was interrupted and the sample was photographed under an MBS-10 microscope equipped with an image digitizer. The backlight was adjusted so that to highlight the entire coating surface. In so doing, the uncoated patches were dark (Fig. 3b). The number of cycles to coating failure was determined from the relationship $N^* = 4Atmn$, where t is the total test time.

The main tests were preceded by preliminary tests conducted at the load $P = 4$ N to identify the most resistant out of the studied coatings. The coating types and test results are given in Table 1.

The main tests were performed on nanosized Al_2O_3 – ZrO_2 coatings with amorphous and nanocrystalline structure ($\sim 6:1$ phase ratio) synthesized by low-temperature thermal decomposition of isomeric Al and Zr carboxylates. Thermolysis involved a two-stage treatment: slow ($\sim 80^\circ\text{C min}^{-1}$) heating to 500°C and additional an-

nealing at 600°C (for 5 min). The ratio of metals in the initial film-forming solution was 1Zr : 1.3Al.

The selected coating was tested under the same conditions but with a higher load varied from 10 to 30 N. The number of cycles to microscopic coating failure ranged from 1.3×10^7 (for a load of 30 N) to 2.2×10^7 (for a load of 10 N). The friction coefficient in all tests did not exceed 0.1.

7. EXPERIMENTAL AND THEORETICAL RESULTS

Modeling was performed with the following experimentally obtained input parameters: the elastic moduli of the coating—148 MPa, substrate—110 MPa and steel counterbody—210 MPa, the coating thickness of 140 nm, the average roughness curvature radius of $9 \mu\text{m}$, the average roughness period given above, the coefficient of friction assumed to be 0.1 in all calculations for generality, and the total load on the contact ranging from 10 to 30 N; the load values were used to calculate the average load on a roughness element by Eq. (2) and the number of cycles to spalling for each load value.

Figure 6 shows the distributions of the maximum tangential stresses under a roughness element (the plane of section passes through the center of the contact area and is parallel to the sliding direction) for the minimum (10 N) and maximum (30 N) load values. Note that the stress distribution is close to symmetric due to a small value of the friction coefficient. The figure shows the stress values in the maximum points in the coating. The

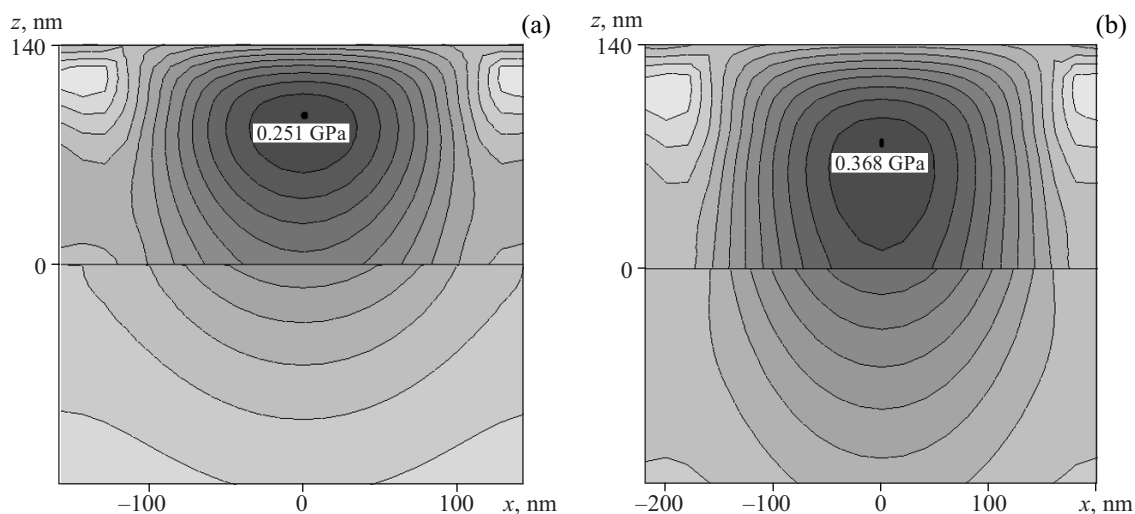


Fig. 6. Distribution of maximum tangential stresses under a roughness element under a load of 10 (a) and 30 N (b) applied to the pin.

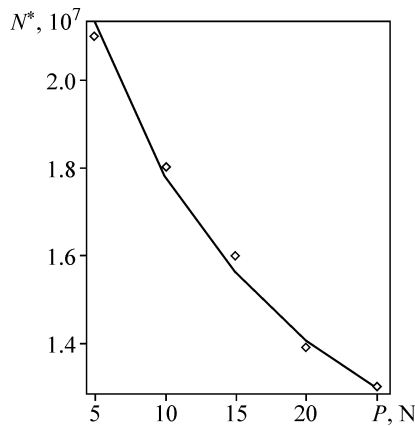


Fig. 7. Load dependence of the number of cycles to spalling. Experimental values (points) and the curve obtained from Eq. (9) with $m = 0.52$, $c = 4.2 \times 10^{16}$.

fact of complete spalling of coatings indicates that despite lower stress concentrations at the coating–substrate interface this region is most susceptible to contact fatigue failure. The amplitude values of the maximum tangential stresses at the interface $\Delta\tau_1$ in the considered load range vary from 68 to 167 MPa.

Obviously, the values of the parameters c and m in Eq. (9) can be calculated using only two values of $\Delta\tau_1$ and N^* obtained for different loads. The result can be verified if there are more data for a sufficiently wide load range. By averaging the results obtained for each pair of points on the experimental N^* versus load curve, we calculated the values of $m = 0.52$ and $c = 1.9 \cdot 10^{16}$. Figure 7 illustrates the experimental values and the curve obtained from Eq. (9) for the calculated values of the parameters. A good agreement of the results proves the adequacy of the model for describing the contact fatigue mechanism of coating spalling.

8. CONCLUSIONS

A method has been developed for the experimental and theoretical study of coating spalling due to contact fatigue damage accumulation in contact with a rough counterbody.

It was shown that the linear damage summation model adequately describes the load dependence of the number of cycles to spalling for thin oxide-based coatings.

Experiments and calculations were performed for the considered substrate–coating composition to estimate the parameters c and m entering the equation that relates the amplitude values of the maximum tangential stresses

arising in sliding friction between a rough counterbody and the coating surface with the number of cycles to coating spalling.

ACKNOWLEDGMENTS

The work was financially supported by the Federal Agency of Scientific Organizations (Reg. No. AAAA-A17-117021310379-5), and partially supported by the Russian Foundation for Basic Research (Project No. 17-58-52030).

REFERENCES

1. Stewart, S. and Ahmed, R., Rolling Contact Fatigue of Surface Coatings—A Review, *Wear*, 2002, vol. 253(11–12), pp. 1132–1144.
2. Zhong-yu, P., Bin-shi, X., Hai-dou, W., and Dong-hui, W., Investigation of RCF Failure Prewarning of Fe-Based Coating by Online Monitoring, *Tribol. Int.*, 2014, vol. 72, pp. 156–160.
3. Goryacheva, I.G. and Torskaya, E.V., A Periodical Contact Problem for a System of Dies and Elastic Layer Adhered to Another Base, *Trenie Iznos*, 1995, vol. 16, no. 4, pp. 642–652.
4. Goryacheva, I.G. and Torskaya, E.V., Modeling of Fatigue Wear of a Two-Layered Elastic Half-Space in Contact with Periodic System of Indenters, *Wear*, 2010, vol. 286(11–12), pp. 1417–1422.
5. Torskaya, E.V., Modeling of Fatigue Damage of Coated Bodies under Frictional Loading, *Phys. Mesomech.*, 2016, vol. 19, no. 3, pp. 291–297.
6. Goryacheva, I.G., *Contact Mechanics in Tribology*, Dordrecht: Kluwer Academic Publ., 1998.
7. Nikishin, V.S. and Shapiro, G.S., *Three-Dimensional Problems of Elasticity Theory for Multilayered Media*, Moscow: VTs AN SSSR, 1970.
8. Ionov, V.N. and Ogibalov, P.M., *Strength of Three-Dimensional Structural Elements*, Moscow: Vysshaya Shkola, 1972.
9. Collins, J.A., *Failure of Materials in Mechanical Design: Analysis, Prediction, Prevention*, New York: Wiley, 1993.
10. Sakharov, V.V., Baskov, P.B., Berikashvili, V.Sh., Ivkina, O.V., Kosov, D.E., Mosyagina, I.V., Frolov, N.N., and Sharipova, M.A., Nanoscale Oxide Surface Modification of Inorganic Materials, *Russ. J. Gen. Chem.*, 2013, vol. 83, no. 11, pp. 2159–2166.
11. Torskaya, E.V., Kurbatkin, I.I., Mezrin, A.M., Morozov, A.V., Murav'eva, T.I., Frolov, N.N., and Sakharov, V.V., Mechanical and Tribological Properties of Nanostructured Coatings Based on Multicomponent Oxides, *J. Friction Wear*, 2013, vol. 34, no. 2, pp. 99–106.
12. Kravchuk, K.S., Torskaya, E.V., Useinov A.S., and Frolov, N.N., Experimental and Theoretical Study of What

- Causes Spallation for Multicomponent Oxide-Based Coatings under Friction Loading, *Mech. Solids*, 2015, vol. 50, no. 1, pp. 52–61.
13. Kablov, E.N., Grashchenkov, D.V., Isaeva, N.V., and Solntsev, S.S., Perspective High-Temperature Ceramic Composite Materials, *Russ. J. Gen. Chem.*, 2011, vol. 81, no. 5, pp. 986–991.
 14. Andreeva, A.V., *Basics of Physical Chemistry and Technology of Composites: Handbook for Students*, Moscow: Radiotekhnika, 2001.
 15. Useinov, A.S., Radzinsky, S.A., Kravchuk, K.S., Zolki-na, I.Yu., Andreeva, T.I., and Simonov-Emelyanov, I.D., Physical and Mechanical Properties of Siloxane Coating on Polymer Substrates, *Plast. Massy*, 2012, no. 4, pp. 14–18.
 16. Goryacheva, I.G., Torskaya, E.V., Kornev, Yu.V., Grigoriev, A. Ya., Kovaleva, I.N., and Myshkin, N.K., Theoretical and Experimental Study of the Mechanical Properties of Bicomponent Metal Vapor Deposited Coatings, *J. Friction Wear*, 2015, vol. 36, no. 3, pp. 262–265.
 17. Sachek, B.Ya. and Merzin, A.M., Studies of the Performance Characteristics of Epilaminized Materials under Conditions of Dry Friction, *J. Machin. Manufact. Reliab.*, 2015, no. 1, pp. 40–45.